AN EFFICIENT METHOD FOR MEASURING DISCHARGE OF A RIVER WITH SHORT-TERM REVERSED FLOWS

By

Bill Kasch

A thesis submitted in partial fulfillment of

the requirements for the degree of

Master of Science

(Civil and Environmental Engineering)

at the

UNIVERSITY OF WISCONSIN-MADISON

2015

Abstract

An efficient method for estimating discharge of rivers with short-term reversed flow is developed using entropy-based velocity distribution equations. The proposed method, called adaptive horizontal entropy method (AHEM), allows an adaptive range of velocity sampling using a stationary horizontal acoustic Doppler current profiler (HADCP). In AHEM, the mean velocity is related to the averaged HADCP velocities in a linear relationship after establishing velocity distribution parameters. To test the performance of AHEM in measuring short-term reversed flows, AHEM is deployed at Yahara River in Wisconsin, and the estimated discharges are then compared with measurements by a moving boat vertical ADCP. The results show that it performed well for short-term reversed flows. Root mean square error of AHEM estimation is 0.37 m^3/s, the mean relative error is 13.1% and the coefficient of determination is 0.984. In comparison with the well-established index velocity method, AHEM yielded slightly lower errors, indicating reasonable accuracy. AHEM can reliably estimate discharge using a flexible HADCP data coverage area without recalibration and also adapt to changes in the velocity distribution by using fit velocity distribution parameters.

An efficient method for measuring discharge of a river with short-term reversed flows

1. Introduction

Measuring discharge of rivers with short-term reversed flows is challenging due to the rapid changes in flow direction and magnitudes (Herschy, 2009). The time of short-term reversed flows are typical from several minutes to a few hours (Sorensen et al. 2004; Kirillin et al. 2014). They are different from reversed flows driven by tidal effects in estuarine rivers since they have a time period around 12 hours (Sorensen et al. 2004). One possible driving force for short-term reversed flows in rivers is wind-induced standing waves which are called seiches. (Germain, 2013). A study has found bidirectional flows occurred in a river connected to an inland lake with seiching events, and that the time period for flow reversal was less than 30 minutes (Germain, 2013). The small time period of short-term reversed flows complicates the hydrodynamic features of flow structure. For example, studies show that not only the velocity profiles vary constantly when flow accelerates and decelerates, but also eddies and water moving across channel can be generated when flow changes direction frequently (Sorensen et al. 2004). Therefore, an efficient method that allows fast, reliable and continuous recording of the rapid variations in the flow regime is needed in order to measure the discharge of short-term reversed flows.

Discharge in rivers with short-term reversed flows can be quickly measured by towing an acoustic Doppler current profiler (ADCP) across the channel (Turnipseed and Sauer, 2010; Mueller et al. 2013). The ADCP is able to measure flow velocities and depths along the cross section using downward looking acoustic Doppler sensors (Mueller et al. 2013), and then the discharge is calculated by the velocity-area method (Turnipseed and Sauer, 2010). Although

simple and fast measurement can be achieved, the moving-boat ADCP method still has certain limitations. First, it requires an operator on site, which makes this method impossible for continuous monitoring of discharge variations for a long period of time. Second, this method does not work in wide rivers when the sampling time of moving the device across the channel section exceeds the time period of reversed flows. Overall, direct measurement using moving-boat ADCP is not capable of providing continuous and reliable discharge measurement in rivers with short-term reversed flows.

For continuous measurement, the index velocity method is commonly used to compute the discharge of rivers with reversed flows (Levesque and Oberg, 2012). The index velocity method differs from the traditional stage-discharge method by separating velocity and area into two ratings –the index rating and the stage-area rating, and the discharge is calculated as the product of the two outputs (Levesque and Oberg, 2012). A stage sensor and an index velocity meter, which is usually an acoustic Doppler velocity meter (ADVM), are installed on site to provide data for continuously computing discharge (Levesque and Oberg, 2012). Although the index velocity method has been successfully applied in estuarine rivers with reversed flow (Ruhl and Simpson, 2005; Hoitink et al., 2009; Levesque and Oberg, 2012), there still remains a concern that rapid temporal variations in short-term reversed flows would break the established regression-based rating relations, and consequently frequent recalibration will be required (Morse et al., 2010). Therefore, a versatile methodology with a proven performance in constantly changing flow conditions needs to be considered in order to make reliable measurement of short-term reverse flows.

Entropy-based discharge estimation shows promises to be applied in rivers with short-term reversed flows based on its reliable performance in measuring estuarine rivers (Chen and

Chiu, 2002; Bechle et al. 2014). The method is derived from the probability theory and the principle of maximum entropy (POME) (Chiu, 1987; 1988), and is able to estimate discharge by computing the cross-sectional velocity distributions from a few sampling points, usually obtained by a vertical acoustic Doppler velocity profiler (VADCP). In addition, the velocity distribution equations are rearranged to establish a linear relationship between the mean velocity and the maximum velocity of the cross section (Chiu and Said, 1995; Xia, 1997; Chiu, 1987 and 1988; Chiu and Tung, 2002; Moramarco, Saltalippi and Singh, 2004; Marini et al. 2011). This linear relationship expedites the discharge estimation since a single measurement at the location of maximum velocity is sufficient for computing discharge. Furthermore, extensions of this relationship have also been made and discharge can thus be calculated by using velocities at other more flexible locations than only at the location of the maximum velocity. These include a single point surface velocity measured above the maximum velocity (Chiu et al., 2005; Fulton and Ostrowski, 2008), a vertical strip of velocities measured from a stationary upward looking ADCP (Morse et al, 2010), and a set of surface velocities along the cross section (Bechle and Wu, 2014). To summarize, the entropy-based method calculates discharge based on a theoretically sound equation with a small number of sampling points. It has a versatile performance that adapted well with variations in estuarine reversed flows (Chen and Chiu, 2002; Bechle et al. 2014). Therefore, it is of great interest to apply the entropy-based method for short-term reversed flows.

One major challenge, nevertheless, exists in applying the entropy-based method to estimate discharge of rivers with short-term flow reversals. Due to the rapid variation and generated eddies and mixings in flow structures of short-term reversals (Sorensen et al. 2004), it is likely that a certain portion of sampling points collected using a velocity measurement device

such as an ADCP will have a significant amount of noise and thus cannot be used (Levesque and Oberg, 2012). In addition, site and equipment limitations such as channel dimensions exceeding the equipment range, or interferences from debris and large particles, could also lead to the situation that valid sampling data could only be obtained from a certain portion of the channel. This makes the discharge estimation difficult for two reasons: first, the measurable range may exclude key data such as the maximum velocity; second, the range is a dynamic variable as it constantly changes with different flow conditions. Therefore, it is desired to have a method that is able to adapt to different spatial data coverages. Recently, Bechle and Wu (2014) have proposed a flexible sampling coverage in surface velocity measurement in estuarine rivers. Yet it remains uncertain if the flexible scheme can be applied in short-term reverse flows. Therefore, the challenge associated with limited sampling coverage needs to be resolved in order to measure discharge of rivers with short-term reversed flows.

The purpose of this paper is to develop an efficient method for estimating discharge of rivers with short-term reversed flow. The proposed method allows an adaptive range of velocity sampling using a stationary horizontal acoustic Doppler current profiler (HADCP), and the method is called adaptive horizontal entropy method (AHEM). In AHEM, the entropy-based velocity distributions by Chiu (1987) are modified and the mean velocity is related to the averaged HADCP velocities in a linear relationship. To test the performance of AHEM in measuring short-term reversed flows, AHEM is deployed at the Yahara River in Wisconsin. The estimated discharges are then compared with measurements by a moving boat vertical ADCP.

The paper is structured as follows. Section 2 explains the AHEM equations with derivations of entropy relations. Section 3 introduces the study site and field measurement. Section 4 presents the results of parameter determination and discharge estimates. Section 5

discusses the impact of different spatial data coverages on accuracy and recommendations for implementing AHEM. Finally, conclusions are provided in section 6.

2. Method

2.1 Mean velocity relationships

2.1.1 Relation between mean and maximum velocity

The relation between mean and maximum velocity in an open channel cross section is developed with the formulation of the entropy-based velocity distributions, as presented in Chiu (1988). Chiu's derivation of velocity distribution equations is based on the postulate that a system under a steady equilibrium condition tends to maximize entropy (Chiu, 1988). Entropy is a measure of information, choice, and uncertainty (Shannon, 1948) and is related to the probability of occurrence of an event. Events with lower probability of occurrence have higher entropy and events with higher probability have lower entropy. For example, a system in which only a few states are possible has low entropy because there are less outcomes and therefore, less information in the system. By applying the concept of probability and the maximization of Shannon entropy, Chiu (1988) derived the channel cross-sectional velocity distribution as a function of the maximum velocity

$$\frac{u}{u_{max}} = \frac{1}{M}\ln\left[1 + (e^{M} - 1)\frac{\xi - \xi_o}{\xi_{max} - \xi_o}\right] \quad (1)$$

where M is a dimensionless entropy parameter for characterizing the uniformity of various patterns of the velocity distribution. ξ is the isovel function of the channel cross section. An isovel is a contour of equal velocity, such that it decreases away from the location of the

maximum velocity at ξ_{max} to the location of the minimum velocity at ξ_0 (Chiu and Chiou, 1988; Chiu and Lin, 1983). The isovel equation was provided by Chiu (1988) as

$$\xi = \frac{y(x)}{D(x)-h}\left(1-\frac{|x-x_{max}|}{B_i}\right)^{\beta_i}\exp\left[\beta_i\frac{|x-x_{max}|}{B_i}-\frac{y(x)}{D(x)-h}+1\right] \quad (2)$$

where x is the horizontal location with x_{max} as the horizontal location of the maximum velocity u_{max}; $y(x)$ is the vertical distance from the bed; $D(x)$ is the water depth and h is the depth to u_{max}; B_i is the horizontal distance from x_{max} to the left (B_L) or right (B_R) bank determined by facing the downstream direction; β_i is a shaping parameter of the isovel distribution for the left and right sides of x_{max} respectively (β_L and β_R). See Figure 1 for an illustration of the aforementioned parameters with $\beta_L = \beta_R = 1$. Increasing the value of β will cause velocities to decrease more sharply from x_{max}.

The relation between the mean velocity $\bar{u}$ and the maximum velocity u_{max} can be expressed as a function of the entropy parameter M (Chiu and Said, 1995)

$$\frac{\bar{u}}{u_{max}} = \frac{e^M}{(e^M-1)} - \frac{1}{M} = \Phi(M) \quad (3)$$

Eq. (3) has been validated by several past studies, including Xia (1997), Chiu et al. (2002), Chiu and Tung (2002), Chiu and Chen (2003) and Moramarco et al. (2004). This relation also shows that higher values of M represent more uniform velocity distributions, as M approaches infinity, Φ approaches unity, yielding $\bar{u} = u_{max}$; as M decreases, Φ approaches zero, resulting in a sharp velocity distribution. With Eq. (3), the mean velocity can be quickly estimated by knowing the entropy parameter M and the maximum velocity.

3.2.1.2 Derivation of mean velocity as a function of mean HADCP velocity

In this paper, the Adaptive Horizontal Entropy Method (AHEM) is developed by extending the entropy concept to relate the velocity distribution and the HADCP measured velocity. The entropy equations are rearranged in the following steps to express mean velocity ($\bar{u}$) as a function of average HADCP velocity ($\bar{u}_H$).

First, ξ_H is determined by inserting the vertical position of the HADCP, y_H, into Eq. (2)

$$\xi_H = \frac{y_H}{D(x)-h}\left(1-\frac{|x-x_{max}|}{B_i}\right)^{\beta_i}\exp\left[\beta_i\frac{|x-x_{max}|}{B_i}-\frac{y_H}{D(x)-h}+1\right] \tag{4}$$

Then, substituting ξ_H into Eq. (1) yields estimated subsurface velocity at locations of HADCP measurement, u_H

$$u_H = u_{max}\frac{1}{M}\ln\left[1+(e^M-1)\frac{\xi_H-\xi_o}{\xi_{max}-\xi_o}\right] \tag{5}$$

Next, u_{max} is solved in Eq. (5) and inserted into Eq. (1)

$$u = \frac{u_H\frac{1}{M}\ln\left[1+(e^M-1)\frac{\xi-\xi_o}{\xi_{max}-\xi_o}\right]}{\frac{1}{M}\ln\left[1+(e^M-1)\frac{\xi_H-\xi_o}{\xi_{max}-\xi_o}\right]} \tag{6}$$

Eq. (6) allows the velocity at any point in the channel be expressed in terms of u_H. This equation estimates velocity distribution when u_{max} cannot be measured. Furthermore, the mean velocity can also be related to u_H by solving Eq. (5) for u_{max} and inserting it into Eq. (3)

$$\bar{u} = \frac{u_H M \left(\frac{e^M}{(e^M - 1)} - \frac{1}{M}\right)}{\ln\left[1 + (e^M - 1)\frac{\xi_H - \xi_o}{\xi_{max} - \xi_o}\right]} \tag{7}$$

Eq. (7) relates the mean velocity to any HADCP measurement. Therefore, the flow discharge can be estimated based on a single-point measurement at HADCP depth. In addition, it has been shown that entropy-based discharge estimates can be improved by using spatially-averaged velocity measurements instead of single-point velocities (Bechle and Wu, 2014). The spatially-averaged HADCP velocity is thus incorporated into the mean velocity expression. First, by integrating Eq. (5) over the HADCP measurement range from X_L to X_R, the average HADCP velocity, $\bar{u}_H$ is expressed as

$$\bar{u}_H = \frac{u_{max}}{M} \frac{\int_{X_L}^{X_R} \ln\left[1 + (e^M - 1)\frac{\xi_H - \xi_o}{\xi_{max} - \xi_o}\right] dx}{\int_{X_L}^{X_R} dx} \tag{8}$$

Then solving Eq. (8) for u_{max} and substituting it into Eq. (3) yields

$$\frac{\bar{u}}{\bar{u}_H} = M[\frac{e^M}{(e^M - 1)} - \frac{1}{M}] \frac{X_R - X_L}{\int_{X_L}^{X_R} \ln\left[1 + (e^M - 1)\frac{\xi_H - \xi_o}{\xi_{max} - \xi_o}\right] dx} = \Omega \tag{9}$$

Finally, discharge is expressed as

$$Q = \Omega \; x \; \bar{u}_H x \; A \tag{10}$$

where A is cross sectional area. Eq. (9) allows quick estimation of the mean velocity from the average of HADCP measured velocities through the parameter Ω. In other words, the mean velocity is a function of M, β, x_{max}, h/D and X_L, X_R, $\bar{u}_H$. The first four variables are entropy parameters of the channel (Bechle and Wu, 2014), and the last three are values from the HADCP

measurements. The integral in the denominator of Eq. (9) cannot be evaluated analytically and needs to be integrated numerically, and if two values of B (B_L and B_R) and two values of β (β_L and β_R) are used, piecewise evaluation for the left and right sides will also be performed. A is obtained from a stage-area relationship.

2.3 Entropy parameters

Entropy parameters M, h, x_{max} and β are determined from velocity and water depth measurement over a channel cross section. Most conventional entropy-based discharge estimation methods assume those entropy parameters to be constant over varying flow conditions. For example, Chiu et al. (2005) found that M was stable for steady flows over 20 year periods. However, for tidal streams, M varied in different phases (Chen and Chiu, 2002). In addition to M, x_{max}, the location of maximum velocity, also changed considerably over periods of tide-induced bidirectional flow (Bechle and Wu, 2014). Therefore, in determining the value of those entropy parameters, considerations of their variations in different discharge conditions need to be particularly taken into account.

M is calculated through a residual minimization procedure. For each transect, Eq. (2) is used to calculate velocities at measured locations, and the values are compared with corresponding measured velocities. M is adjusted until the total residual sum of squares between calculated and measured velocities reaches below a preset tolerance value. For a set of data with a range of discharge, if M remains stable, M is determined as the average of all M values. On the other hand, if M varies significantly, then M is determined with separate regressions to relate to the average HADCP velocity (Bechle and Wu, 2014).

The normalized vertical location of the maximum velocity, *h/D*, is obtained directly from the velocity distribution measurement of the cross section. Similar to the determination of *M*, the average of all *h/D* values is used for discharge estimate if *h/D* remains stable over a range of discharges; otherwise, this parameter will be related the average of HADCP velocities with separate regressions.

The horizontal location of the maximum velocity, x_{max} is assumed to coincide with the horizontal location of the maximum HADCP velocity. This assumption is verified by comparing x_{max} measured by the HADCP and VADCP. Also, theoretically, this assumption is true for high values of β or when *D(x)* does not vary significantly near x_{max}. In Eq. (2), β is associated with the $\frac{|x-x_{max}|}{B_i}$ term, so if β is large enough such that it dominates over the $\frac{y}{D(x)-h}$ term or *D(x)* is held constant, u_{Hmax} will coincide with x_{max} regardless of vertical position *h*.

Values of the shaping parameter β are determined using the residual minimization procedure. Two values of β (β_L and β_R), one each for the left and right sides of the cross section, are assumed first. Then the maximum HADCP velocity, $u_{Hmax,}$ is substituted into Eq. (6) to calculate velocities at each HADCP measurement location, and the calculated velocities are compared with the HADCP measurement. Values of β are adjusted until the total residual sum of squares is minimized. An example of fitting β values is demonstrated in Figure 2.

3. Field Data

3.1 Study Site

The study site, illustrated in Figure 3, is located on the Yahara River between Cherokee Marsh and Lake Mendota in Dane County, Wisconsin. The cross section is located at 10 meters

downstream of the State Highway 113 Bridge. The cross section is 19.2 meters wide with a maximum depth of 2.2 meters.

Short-term reversed flows are likely to occur when wind-induced seiching events occur in the lake, since the study site is located near the inlet of Lake Mendota. Figure 4 shows a time series of the discharge, river stage, wind direction and speed for a four-hour period in the study site. The first observation is that reverse flow occurred at the cross section when wind from the SSW direction reached high speeds. For example, as shown in Figure 4, at 2:40pm the SSW wind reached a speed as high as 7m/s, and shortly after at 2:50pm, negative discharge was observed; similarly, at 4pm the discharge was negative when the SSW wind reached a high speed of 6.5m/s. The SSW wind pushed water of Lake Mendota towards the northeast inlet, and the water moved upstream through the Yahara River to Cherokee Marsh, resulting in reversed flow. Nevertheless, high speed SSW wind could not explain all flow reversal events in the Yahara River, as the negative discharge at 3:20pm occurred when the wind speed was low. Overall, the short-term reversed flows in rivers are likely to occur when strong wind induce seiches in the connected lake, though its complexity and unsteadiness can hardly be explained by a single mechanism.

The second observation is that the discharge fluctuation affected the river stage. As for the period between 3:30pm to 4:30pm, stage tended to increase as discharge decreased, and stage decreased as discharge increased. Water accumulated near Cherokee Marsh when the flow reversed, causing the increase in river stage, and after wind speed decreased, flow occurs in the downstream direction and water is released from Cherokee Marsh, resulting in a stage decrease. Yet for other time periods, no apparent trend was observed; thus a correlation between the stage and discharge cannot be established.

3.2 Field Measurement

Field measurements were taken at the study site on four days: August 30th, September 19th, October 15th, and October 24th, 2012. The October 24th data set was used for validation of AHEM, and the prior data sets were used for calibration. For the combined data set, discharge ranged from -7.30 to 3.97 m^3/s, and the maximum flow depth varied slightly between measurements from 2.12 to 2.22 m. A summary of data statistics is provided in Table 1.

The measurement instruments included a horizontal acoustic Doppler current profiler (HADCP) and a vertical acoustic Doppler current profiler (VADCP). The HADCP was a Teledyne RDI Channelmaster 1200 kHz model. It was attached to a submerged rigid frame located on the right bank and at 0.4 m below the water surface. The HADCP measured flow depth and velocities across the channel section at an interval of 0.25 m. The HADCP had a blanking distance of 0.5 m and a sampling frequency of 1 Hz. A 2-min averaging interval was used to smooth the HADCP data.

The VADCP was a Sontek River Surveyor S5 model. It was pulled across the channel using a rope and two pulleys fixed on opposite sides of the cross section (Figure 3) to measure the three-dimensional velocity profiles and the channel bathymetry. Velocity data were collected with a vertical beam at 1MHz frequency, and the cell size ranged from 0.02 to 0.5m, depending on the flow depth and boat moving velocity. Depths were measured by bottom-tracking. Each transect took approximately 2 minutes to ensure sufficient sampling in the vertical direction. For the rapid variations in short-term reversed flow, only a single transect could be obtained before the discharge changed significantly. Therefore, averaging over successive transects, as recommended by USGS flow measurement standards (Mueller et al. 2013), could not be applied in this condition. In consideration of the errors, USGS (2005b) has a 12% mean coefficient of

variation (CV) for mean velocities of steady flows less than 0.25 m/s. This 12% CV would also be expected in the VADCP measurement since the mean velocities in the data set were less than the 0.25 m/s threshold, and the unsteady reversals could even add more uncertainties.

4. Results

4.1 Parameter Determination

Entropy parameters M, h, x_{max} and β are determined from measurement data of the velocity and water depth distributions of a channel cross section. As emphasized in Section 2, the possible variation of entropy parameters due to short-term river reverse flows is carefully taken into account when those parameters are determined.

The entropy parameter M is calculated from the VADCP calibration data sets for the negative and positive flow regimes obtained on September 19th and October 16th, respectively. Figure 5 shows the velocity profiles based on measurement and calculation for high magnitude positive and negative discharges. It has been found that an M value of 2 minimized the errors between calculated and measured velocities. In the analysis of discharge results, M value of 2 also shows reliable discharge estimates and does not cause significant systematic error over a specific discharge range. Therefore, M is determined at a constant value of 2 for all estimates.

The parameter concerning the vertical location of the maximum velocity, h/D demonstrated a consistent value from the VADCP data over the entire observed discharge range. The vertical location of the maximum velocity, h is determined by averaging the vertical coordinates of the top 5% of VADCP velocities. The results are shown in Figure 6a. A gradual increase in h/D can be observed from negative to positive flows, however, the overall change from negative to positive flows is very small. The average h/D is 0.394 for flows below -3 m^3/s

and 0.404 for flows above 2 m^3/s. This change has a very small impact on results, so *h/D* is assumed constant at 0.4 in all discharge estimates.

For the parameter concerning the horizontal location of the maximum velocity, x_{max}, the assumption that the horizontal locations of u_{Hmax} coincide with those of u_{max} is verified. x_{max} is determined by averaging the x-coordinates of the top 5% of velocities measured by the VADCP, while x_{Hmax} is determined by averaging those measured by the HADCP. The estimates of x_{max} and x_{Hmax} are compared over the full range of observed discharges. Results are shown in Figure 6b and 6c and summarized in Table 2. Similar patterns in x_{max} and x_{Hmax} are exhibited. For non-low flows, which have discharge either below 3 m^3/s or above 2 m^3/s, both data sets show that x_{max} and x_{Hmax} are consistent and stable at values of 12.5 and 10.7 meters, respectively. This agreement in x_{max} and x_{Hmax} implies that the two-dimensional velocity distribution tends to be stabilized with high flow magnitudes. As illustrated in Figure 7, for positive and negative flows, velocity distributions are well-defined as velocities decrease with horizontal positions moving from the x_{max} towards the bank. Therefore, for non-low flows, the estimates of x_{max} from VADCP and x_{Hmax} from HADCP are expected to be consistent. Nevertheless, for low flows, great variability in x_{max} at near-zero discharges is observed for both HADCP and VADCP data sets as shown in Figure 6. In Figure 7, the velocity distribution is also poorly-defined with multiple high-velocity areas scattered throughout the cross-section. In this low flow case, the x_{Hmax} estimates from HADCP are expected to have significant deviations from x_{max}. To summarize, the assumption that x_{max} can be replaced by the value of x_{Hmax} tends to be more reliable for flows with high magnitudes than low flows, and larger errors are expected for the latter case.

The shaping parameters β_L and β_R are calculated from each HADCP data set. The mean value of β_L is 14.7 with a standard deviation of 8.3. β_R has a mean value of 12.5 and a standard

deviation of 11.6. β_L does not exhibit a significant trend over discharge ranges, while $\beta_{R,}$ on the other hand, tends to increase by a factor of 2 when transitioning from positive to negative discharges. This high value of β_R comes from the sharp velocity distribution on the right side of the channel when x_{max} is located closer to the right bank for negative flows. Figure 8 shows an example of the change in velocity distributions as β varies. From 12:32pm to 2:03 pm., the maximum velocity does not change while the discharge increases; to account for this increase, a wider velocity distribution with a smaller β is used. Overall, Table 3 summarizes the mean and standard deviation of β_L and β_R for positive and negative discharges that are used in the discharge estimation.

Lastly, a stage-area relationship was developed for use in Equation 10. Cross sectional areas were measured with the VADCP, and stage was measured with the HADCP. The stage-area relationship was linear: A = 19.2S+20.8, where S is stage. Estimated areas had a root mean square error (RMSE) of 0.38 m^2 and mean relative error of 1%, indicating a good fit.

4.2 Discharge Estimates

Results of AHEM discharge estimates are compared against the moving-boat ADCP measured discharge, and analyzed quantitatively using statistical measures including the root mean square error (RMSE), the relative error (RE) and the coefficient of determination (R^2). The validity of these measures is assessed separately for the entire data set and validation data set of October 24th. For all data, RMSE of AHEM estimation is 0.37 m^3/s, the mean RE is 13.1% and the R^2 value is 0.984. These results are compared with values from the literature. First, RMSE is normalized by the magnitude of discharge and became 3.3%, which is compared favorably to the range of 4.6% to 7.3% as reported in Chiu (2002). Second, RE is assessed by calculating the coefficient of variation of normalized RMSE (CV(RMSE)). For discharge of

magnitude less than 2 m^3/s, CV(RMSE) falls within the CV range of 5 to 27% reported for discharge measurements during low flows (USGS, 2005; Rehmel, 2007). For discharge less than -4 or greater than 2 m^3/s, RE decreases to within the reported mean CV of 12% (USGS, 2005b), indicating an acceptable error. The R^2 value is also considered reasonable as it compares similarly to studies that used HADCP index velocity methods or traditional entropy methods to estimate tidal flows (Hittle et al., 2001; Chiu, 2002). For the validation data set obtained on October 24th, RMSE, RE, and R^2 values were 0.26 m^3/s, 19.5%, and 0.91, respectively. These results also compared well with literature values. When normalized by magnitude of discharge, RMSE become 7.1%, which still compares favorably with Chiu (2002). When considering higher discharges, CV(RMSE) approached the reported mean of 12% (USGS, 2005b). For example, for discharge magnitudes above 2 m^3/s, CV(RMSE) was 13.3%.

To examine the ability of AHEM in providing continuous discharge estimation of the short-term reversed flows over a period of time, the estimated discharges are plotted in a time series against the measured discharges from the moving-boat VADCP data, as shown in Figure 9. Three different flow regimes are considered: negative, positive, and transitional. As shown, when the river is oscillating between positive and negative flows, AHEM is able to detect a change in flow direction and provide an appropriate sign and magnitude for the discharge estimate. The mean RE of the estimated discharge time series for the three flow regimes is 9.12 %, 7.24 % and 19.5 %, respectively. The result is reasonable since the transitional flow regime corresponds to small discharge, which is more likely to have large relative errors in comparison to positive and negative flows of large discharges because of smaller values in the denominator. Overall, the AHEM is able to provide continuous discharge for different flow regimes with the short-term flow reversals.

The results of AHEM are also compared to discharge estimates made by other methods, which include the index velocity method, the conventional entropy methods and Chiu's original method. The index velocity method estimates the discharge based on the regression relationship between the cross sectional average velocity and the average HADCP measured velocities. The conventional entropy methods estimate discharge using a single-point measurement with constant entropy parameters. In this study, a single point HADCP velocity, u_H, at the mean location of x_{max} and constant entropy parameters (mean values of x_{max}, β_L, and β_R) are used in the comparison. Chiu's original entropy method (1988) estimates discharge using the established linear relationship between $\bar{u}$ and u_{max}, with the assumption of constant entropy parameters.

The comparisons are shown in Figures 10 to 12. First, the comparison of AHEM and the index velocity method is shown in Figure 10, in which the estimated discharges are plotted against the moving-boat ADCP measured discharges. For both methods, data points are reasonably close to the line representing $Q_{obs} = Q_{est}$. The RMSE and RE of the index velocity method are 0.39 m^3/s and 13.9%, which are slightly higher than those of AHEM. Second, Figure 11a shows discharge estimates from using the single point HADCP velocity at the mean location of x_{max} and constant entropy parameters. Discharges are consistently underestimated, since from Figure 7, if actual u_{max} occurs at a location other than the determined x_{max}, the velocity measured at the determined x_{max} will always provide an underestimate of u_{max}. The RMSE and RE are 0.85 and 25%, and if fit parameters are used instead, as shown in Figure 11b, the RMSE and RE decrease to 0.55 and 17.3%, which are still higher than those of AHEM. Lastly, Figure 12a shows discharge estimates using Chiu's original entropy method (1988). Again, discharge is consistently underestimated and the RMSE and RE are 1.04 and 39.6%. Figure 12b shows the results by using fit entropy parameters, and the RMSE and RE decrease slightly to 1.0 and

39.0%. Overall, the comparison results are summarized in Table 4 for different methods. It is found that the use of fit parameters reduces errors, indicating the importance of accounting for changes in the entropy parameters for short-term reversed flows. In addition, discharge estimated using spatially averaged HADCP data had considerably less error than that of the point-based methods, suggesting the spatial extent of velocity data is important in estimation accuracy.

5. Discussion

Flexible data coverage area is allowed in AHEM discharge estimation, which presents a significant advantage over empirical index velocity methods that would require recalibration. Although the index velocity regression relation can be developed based on different ranges of HADCP data coverage, every change in the range would require re-establishment of the regression. For AHEM, once the entropy parameters are determined, the data coverage can be changed in different flow conditions without recalibration.

To examine the flexibility in spatial coverage, the performance of AHEM is evaluated for varying spatial coverages of HADCP velocity data. As shown in Figure 13, errors from using velocities from different coverage areas are compared for three cases: i) coverage starting with a single point velocity at mean x_{max} (x ~ 11.3m) with 0% coverage and expanding outwards to the left and right banks, ii) starting at a single point near the east bank (x ~ 0.5m) and proceeding towards the west bank, and iii) starting at a single point near the west bank (x~18 m) and proceeding towards the east bank. Overall the results show that errors decrease as spatial coverage increase. Consider the three cases respectively. First, for the coverage area centers at x ~ 11.3 m, RMSE is 0.55 m^3/s for a single point measurement and steadily decreases to a minimum of 0.35 m^3/s at 71% coverage, then rises slightly until reaching full coverage. The

minimum error occurs at 71% coverage because unsteady velocities exist near the banks, where the flow depth is shallow and reflecting surface waves are likely to occur. Second, for the coverage starting from the east bank, the error is very high at the starting point due to the near-bank turbulence. The error decreases as the coverage increases and reaches a reasonable value at 62% coverage, which also corresponds to the point where mean x_{max} is reached. The error then decreases sharply to 71% coverage and remains stable until reaching full coverage. Lastly, for coverage starting at the west bank, the error variation has a similar pattern as that in the second case. It starts high, decreases to a reasonable value at coverage of 44%, which also corresponds to the point where mean value of x_{max} is reached, and then remains stable until full coverage. To summarize, the results show that discharge can be reliably obtained from a number of different data coverage areas, and the minimum errors can be reached by including the location of the maximum velocity and excluding turbulent areas near the banks in the spatial coverage of HADCP.

The analysis of AHEM spatial coverage provides important implication for the design of stream gauging stations, particularly for finding the optimum device location that results in the best spatial coverage. The best spatial coverage should capture the maximum velocity, which indicates that the HADCP should be located such that it captures a range centered at x_{max}. In addition, the best coverage should also avoid regions with high turbulence. To locate those regions, the HADCP can be installed in a temporary test prior to permanent installation, and the region where collected velocities have a high standard deviation can be identified and excluded from the HADCP designed spatial coverage.

Recommendations are made for selecting number and types of instruments as related to addressing the potential for variable parameters. For this study, the horizontal parameters, x_{max}

and β, were observed to vary over discharge regimes and were automatically calibrated from HADCP data. However, the HADCP does not reveal information about the vertical velocity distribution, so M and h could not be determined from HADCP data alone. That is, the spatial limitations of the instrument in turn dictate what parameters can be automatically calibrated. As another example, an upward-looking ADV collects several velocities at various depths and single horizontal location, therefore revealing information about the vertical velocity distribution but not the horizontal. Therefore, a study site should be assessed for variable parameters before selecting equipment. If only x_{max} and β vary, then an HADCP would be more appropriate. Likewise, an upward-looking ADV would be the best equipment if only h changes. If both horizontal and vertical parameters vary, then horizontal and vertical-looking instruments should be used. In general, a greater number of instruments would result in greater accuracy because more parameters could be automatically calibrated, and the 2-D velocity distribution is better approximated. However, additional devices would be more costly and require additional maintenance, so there are tradeoffs between measurement accuracy, costs, and effort. These three factors will need to be evaluated on a continual basis in order to decide the best set up. For example, if a parameter does not change very often and results in minimal deterioration of accuracy, it may be more efficient to recalibrate one instrument seldomly than to purchase and maintain multiple instruments capable of automatic calibration. To summarize, accuracy can be improved by selecting the appropriate number and type of instruments that will address parameter variations. However, it should be determined whether accuracy needs can still be met by neglecting any parameter variations in order to minimize equipment costs and labor associated with maintenance and recalibration.

Concerning the potential channel geometric changes due to frequent flow reversals, an entropy-based flow depth estimation, which is adapted from the flow depth distribution by Moramarco et al (2013), was also evaluated. This method is used if only partial bathymetry can be obtained or bathymetry is suspected to change over the course of discharge estimates. Moramarco et al. (2013) expressed the probability distribution of the water depth along the cross section as a function of the surface velocity. This allows for estimation of the cross sectional area using surface velocity measurements, mean depth for a partial cross section, and W, an entropy parameter describing the uniformity of the depth distribution. W was found to be stable over all transects with a mean value of 3.08 and standard deviation of 0.23. Cross sectional areas estimated through entropy-based flow depth estimation did not differ significantly from areas estimated with the stage-area relationship. The impact on discharge estimates was also insignificant, yielding similar error statistics. Nonetheless, entropy-based flow depth estimation could prove valuable at other sites and should be evaluated when employing AHEM in the future.

6. Summary and Conclusions

In this paper, an efficient method AHEM is developed, which allows fast, continuous and reliable discharge estimation with a flexible data coverage range. AHEM estimates the river discharge using entropy-based equations that relate the mean velocity with the HADCP velocities and four pre-determined parameters. Those parameters include M, which relates to the velocity distribution in the channel cross section, two parameters concerning the location of the maximum velocity, x_{max} and h/D, and the velocity distribution shaping parameter β. The values of those parameters have been determined from field measurement of the cross sectional flow using a moving-boat VADCP and the HADCP.

AHEM was deployed to estimate the discharge of Yahara River in Wisconsin and the results show that it performed well for short-term reversed flows. First in comparison with the well-established index velocity method, AHEM yielded an RMSE and mean RE that were slightly lower than the index velocity method, which indicates that AHEM's accuracy is reasonable. Furthermore AHEM can reliably estimate discharge using a flexible HADCP data coverage areas without recalibration, while for the index velocity method, recalibration is necessary when the spatial measurement range is changed. In addition, in comparison with conventional entropy-based discharge estimates, AHEM resulted in better performance. AHEM is able to adapt to changes in the velocity distribution by using fit entropy parameters and a spatial extent of velocity data, while the conventional methods assume constant entropy parameters and a point-base velocity. Overall, AHEM has been demonstrated an efficient and versatile method for discharge estimation of short-term river reverse flows.

7. References

Bechle, A., Wu, C., Liu, W. and Kimura, N. (2012). Development and application of an automated river-estuary discharge imaging system. *J. Hydraul. Eng. 138*, 327-339.

Bechle, A., and Wu, C. (2014). An entropy-based surface velocity method for estuarine discharge measurement. *Water Resources Research. 50*, 6106-6128.

Chen, Y., and Chiu, C. (2002). An efficient method of discharge measurement in tidal streams. *J. Hydrol. 265*, 212-224.

Chen, Y., and Chiu, C. (2003). An efficient method of discharge measurement based on probability concept. *J. Hydraul Res. 41*(6), 589-596.

Chen, Y., and Chiu, C. (2004). A fast method of discharge estimation. *Hydrol. Processes. 18*, 1671-1684.

Chiu, C. (1987). Entropy and probability concepts in hydraulics. *J. Hydraul. Eng. 113*(5), 583-600.

Chiu, C. (1988). Entropy and 2-D velocity distribution in open channels. *J. Hydraul Eng. 114*(7), 738-756.

Chiu, C., and Chiou, J. D. (1988). Entropy and 2-D velocity distribution in open-channels. *J. Hydraul. Eng. 114*(7), 738–756.

Chiu, C., Hsu, S., and Tung, N. (2005). Efficient methods of discharge measurements in rivers and streams based on the probability concept. *Hydrol. Processes. 19*(20), 3935-3946.

Chiu, C., and Hsu, S.M. (2006). Probabilistic approach to modeling of velocity distributions in fluid flows. *J. Hydrol, 316*(1-4), 28-42

Chiu, C., and Lin, G.F. (1983). Computation of 3-D flow and shear in open channels. *J. Hydraul. Eng. 109*(11), 1424-1440.

Chiu, C., and Said, A.A. (1995). Maximum and mean velocities in open-channel flow. *J. Hydraul. Eng. 121*(1), 26–35.

Chiu, C., and Tung, N.C. (2002). Maximum velocity and regularities in open-channel flow. *J. Hydraul. Eng. 128*(4), 390–398.

Fulton, J., and Ostrowski, J. (2008). Measuring real-time streamflow using emerging technologies: radar, hydroacoustics, and the probability concept. *J. Hydrol. 357*(1), 1-10.

Germain, CA. ST. (2013, March). *Natural processes in an industrialized setting: sedimentary and hydro- dynamics of the Buffalo River, NY.* Poster presented at GSA Northeastern Section 48th Annual Meeting, Bretton Woods, NH.

Hittle, C., Patina, E., and Zucker, M. (2001) Freshwater flow from estuarine creeks into northeastern Florida bay. *United States Geological Survey Water Resources Investigations Report, 4164*.

Hoitink, A. J. F., Buschman, F.A., and Vermeulen, B. (2009). Continuous measurements of discharge from a horizontal acoustic Doppler current profiler in a tidal river. *Water Resources Research. 45*, W11406.

Kirillin, G., Lorang, M. S., Lippmann, T. C., Gotschalk, C. C. and Schimmelpfennig, S. (2014). Surface seiches in Flathead Lake. *Hydrol. Earth Syst. Sci. Discuss. 11*, 13541–13570

Levesque, V., and Oberg, K. (2012). Computing discharge using the index velocity method. *United States Geological Survey Techniques and Methods 3-A23*.

Marini, G., De Martino, G., Fontana N., Fiorentino. M., and Singh, V.P. (2011). Entropy approach for 2D velocity distribution in open-channel flow. *J. Hydraul. Res., 49*(6), 787-790.

Moramarco, T., Saltalippi, C., and Singh, V.P. (2004), Estimation of mean velocity in natural channel based on Chiu's velocity distribution equation. *J. Hydraul. Eng. 9*(1), 42–50.

Moramarco, T., Corato, G., Melone, F., and Singh, V.P. (2013). An entropy-based method for determining the flow depth distribution in natural channels, *J. Hydro. 497*, 176-188.

Morse, B., Richard, M., Hamai, K., Godin, D. Choquette, Y., Pelletier, G. (2010). Gauging Rivers during All Seasons Using the Q2D Velocity Index Method. *J. Hydraul. Eng. 136*(4), 195-203.

Mueller, D. S., Wagner, C. R., Rehmel, M. S., Oberg, K. A., and Rainville, F. (2013). Measuring discharge with acoustic Doppler current profilers from a moving boat. *United States Geological Survey Techniques and Methods 3-A22*.

Rehmel, S.M. (2007). Field evaluation of shallow-water acoustic Doppler current profiler discharge measurements. *Examining the Confluence of Environmental and Water Concerns-Proceedings of the World Environmental and Water Resources Congress*.

Ruhl, C.A., and Simpson, M.R. (2005). Computation of discharge using the index-velocity method in tidally affected areas. *United States Geological Survey Scientific Investigations Report 5004*.

Shannon, C.E. (1948). A mathematical theory of communication. *The Bell System Technical Journal. 27*, 379-423.

Sorenson, J., Sydor, M., Huls, H., and Costello, M. (2004). Analyses of Lake Superior Seiche Activity for Estimating Effects on Pollution Transport in the St. Louis River Estuary under Extreme Conditions. *J. Great Lakes Res. 30*(2), 293-300.

Turnipseed, D.P., and Sauer, V. B. (2010). Discharge measurements at gauging stations. *United States Geological Survey Techniques and Methods 3-A8.*

Xia, R. (1997). Relation between mean and maximum velocities in a natural river, *J. Hydral. Eng. 123*(8), 720-723.

U.S. Geological Survey. (2005). Guidance on the use of RD Instruments StreamPro acoustic Doppler profiler: U.S.Geological Survey, Office of Surface Water Technical Memorandum 2005.05, accessed August 13, 2008, at *http://hydroacoustics.usgs.gov/memos/OSW2005-05.pdf*

8. Tables and Figures

8.1 Tables

Table 1. Measurement summary

Date	8/30/2012	9/19/2012	10/15/2012	10/24/2012
Time	9:10 - 9:55 am	12:20 - 3:00 pm	12:00 - 3:00 pm	1:00 - 5:00 pm
Q_{meas} Range (m3/s)	-3.07 to 0.84	-7.3 to -2.12	1.66 to 3.97	-1.27 to 2.54
Mean Depth (m)	2.16	2.12	2.15	2.22
Mean Xmax (m)	9.36	12.26	10.34	9.15

Table 2. Mean and standard deviations of u_{max} coordinates

	HADCP		VADCP		VADCP	
Q Range (m^3/s)	X_{max} Mean (m)	X_{max} σ (m)	X_{max} Mean (m)	X_{max} σ (m)	h/D Mean (m/m)	h/D σ (m/m)
-7 to -3	12.84	0.83	12.30	0.87	0.394	0.031
-3 to 2	10.84	1.69	9.71	1.01	0.395	0.035
2 to 4	10.76	0.80	10.64	0.77	0.405	0.028

Table 3. Mean and Standard Deviations of β

	Left Beta (B_L)		Right Beta (β_R)	
	Mean	Std. Dev.	Mean	Std. Dev.
Positive Flow	15.8	9.9	6.9	10.7
Negative Flows	14.2	7.2	15.7	10.9

Table 4. Error statistics for entire data set.

	Fit Parameters		Constant Parameters	
Method	RMSE (m3/s)	Relative Error (%)	RMSE (m3/s)	Relative Error (%)
Index	0.39	13.9%	-	-
AHEM	0.37	13.1%	0.41	14.8%
u_H at x_{max}	0.55	17.3%	0.85	25.0%
Maximum [Chiu, 1987]	1.0	39.0%	1.04	39.6%

8.2 Figures

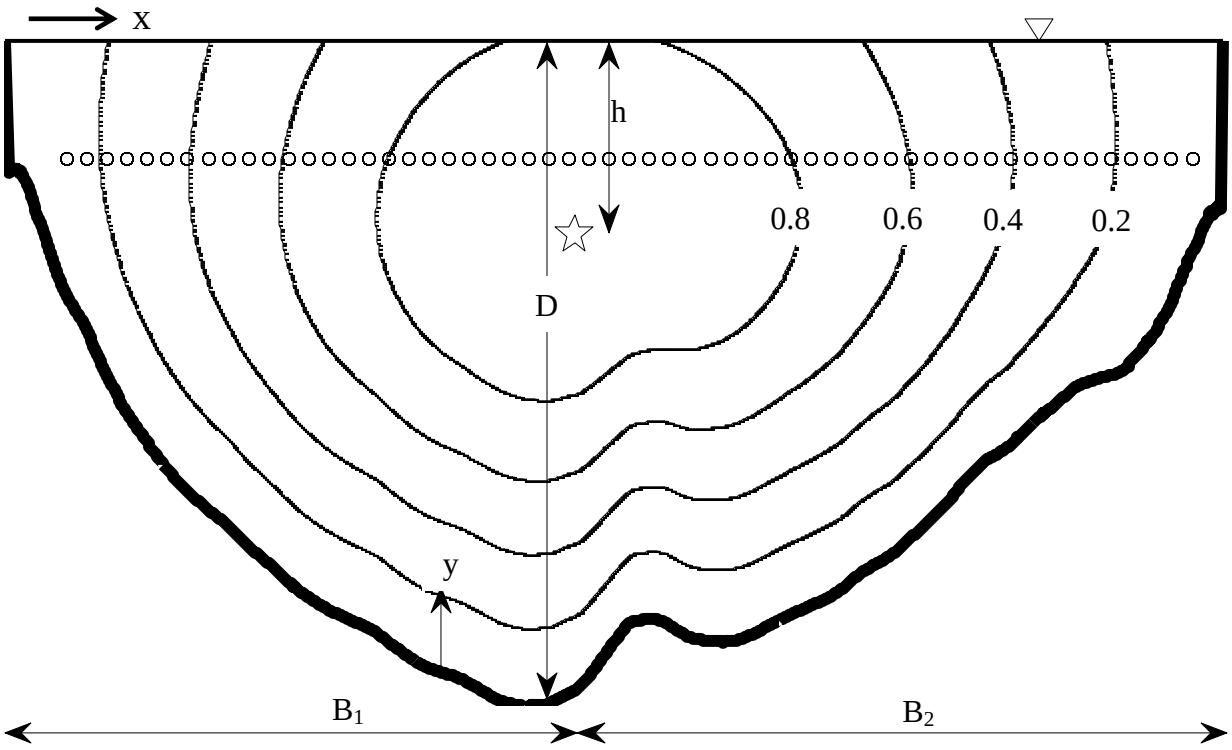

Figure 1: 2-D velocity distribution where M=-2, β=1, and h/D =0.4. HADCP velocities are collected at the same depth and denoted with (o).

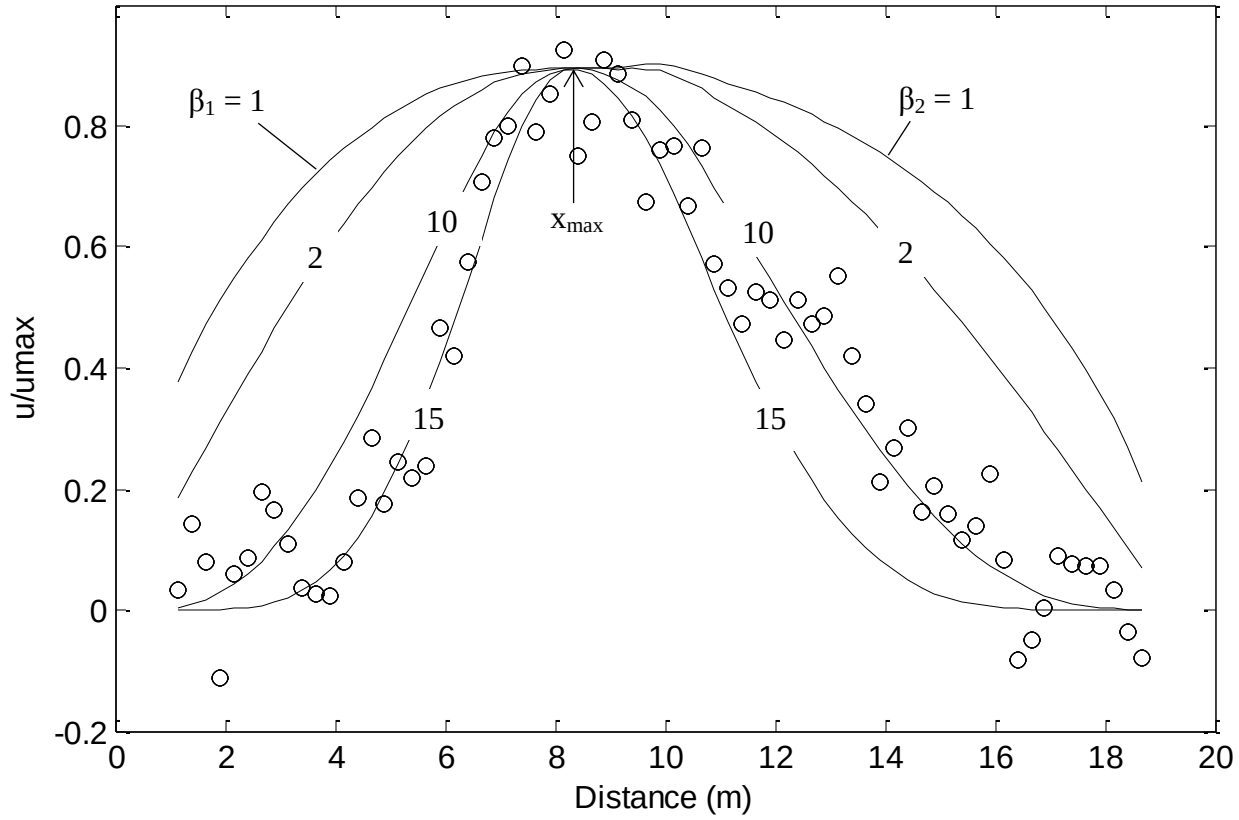

Figure 2: Example of fitting beta values to relative velocity measurements of the HADCP. An increase in beta will narrow the velocity distribution towards the maximum. For this example, $\beta_1 = 15$ and $\beta_2 = 10$.

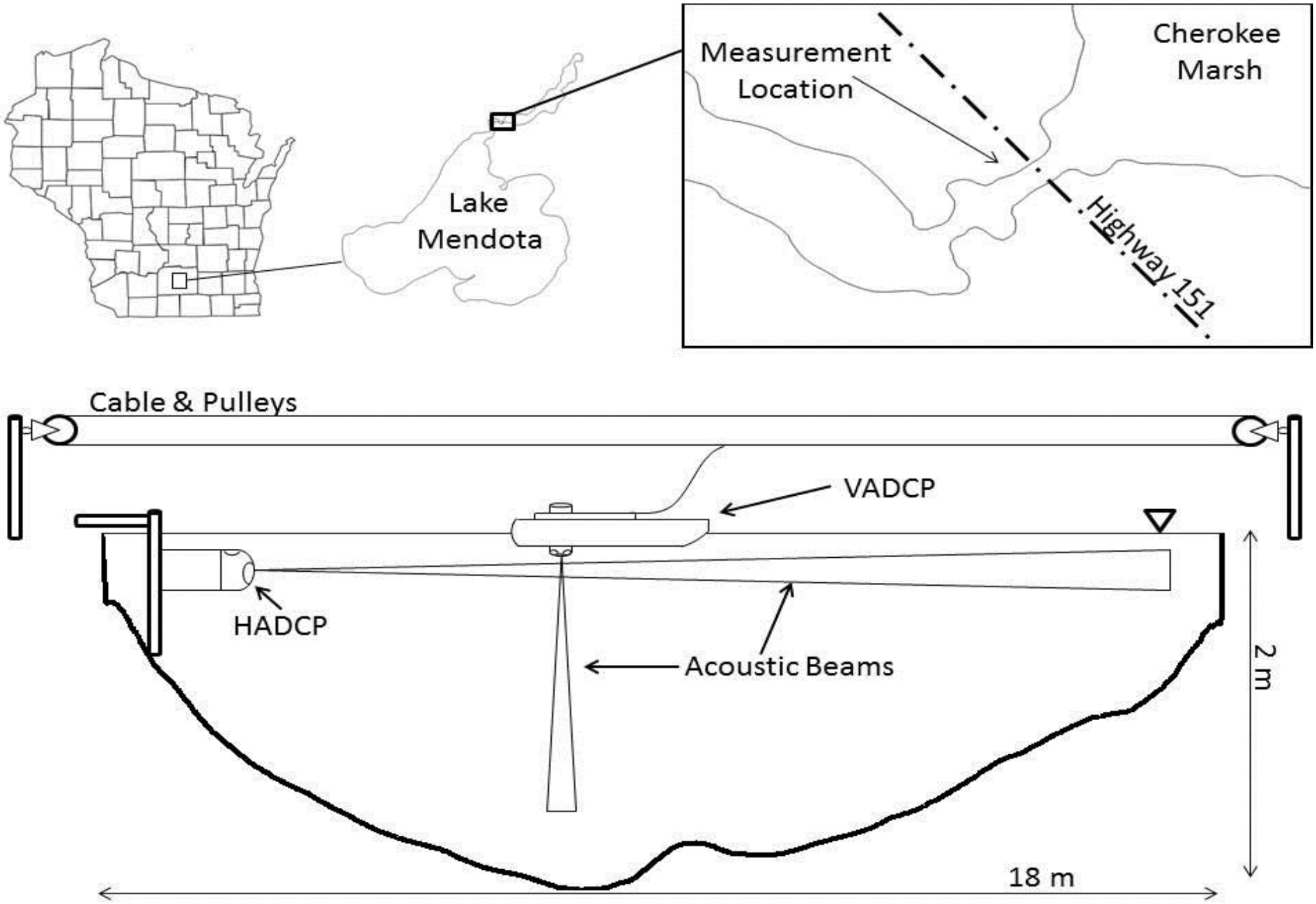

Figure 3: Site location and cross section schematic

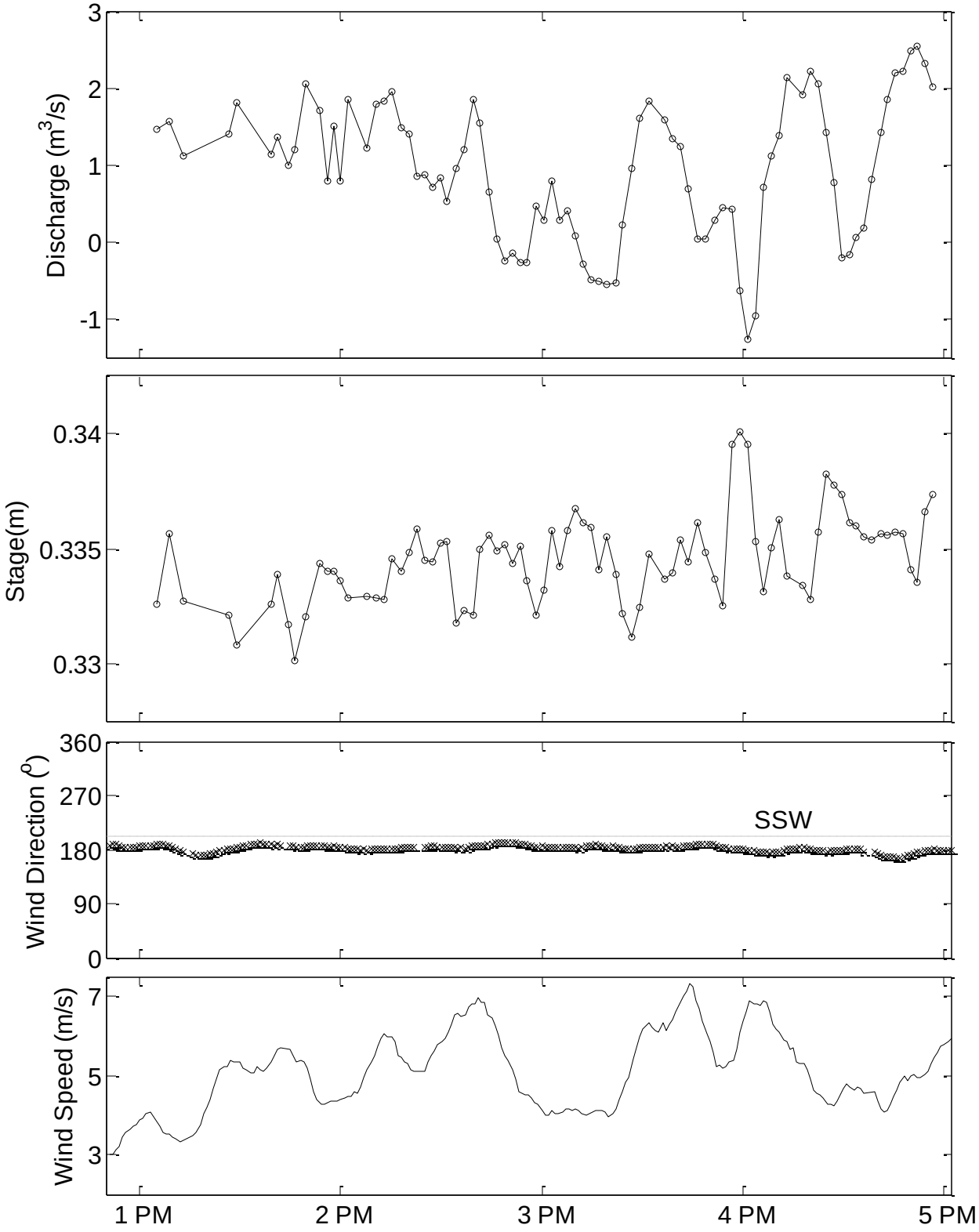

Figure 4: Discharge time series for a reverse flow event.

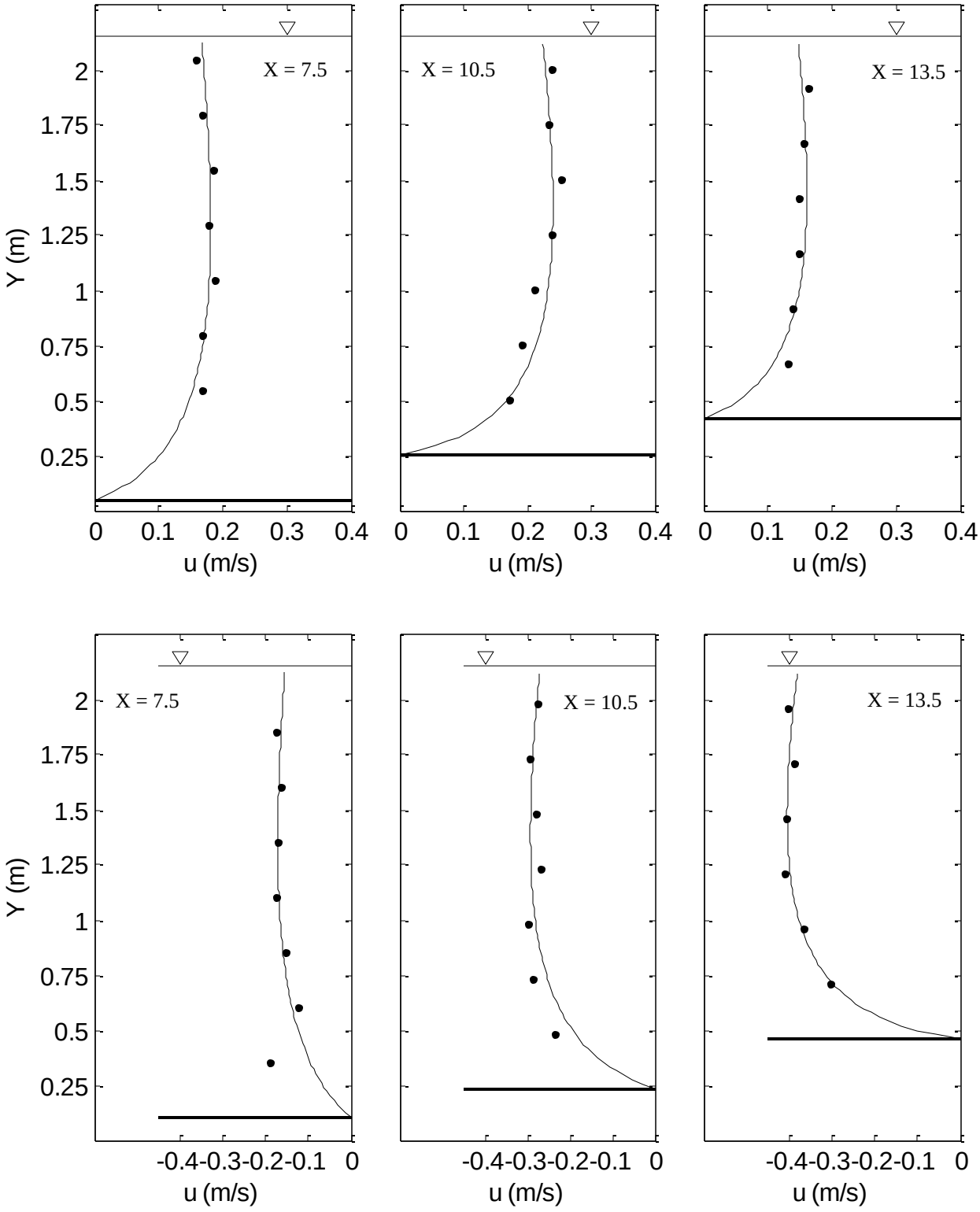

Figure 5: (Top) Fit velocity profiles for positive flows (top, 3 to 4 m^3/s) and negative flows (bottom, -5 to -6.5 m^3/s). M=2, and h/d = 0.4 for all profiles.

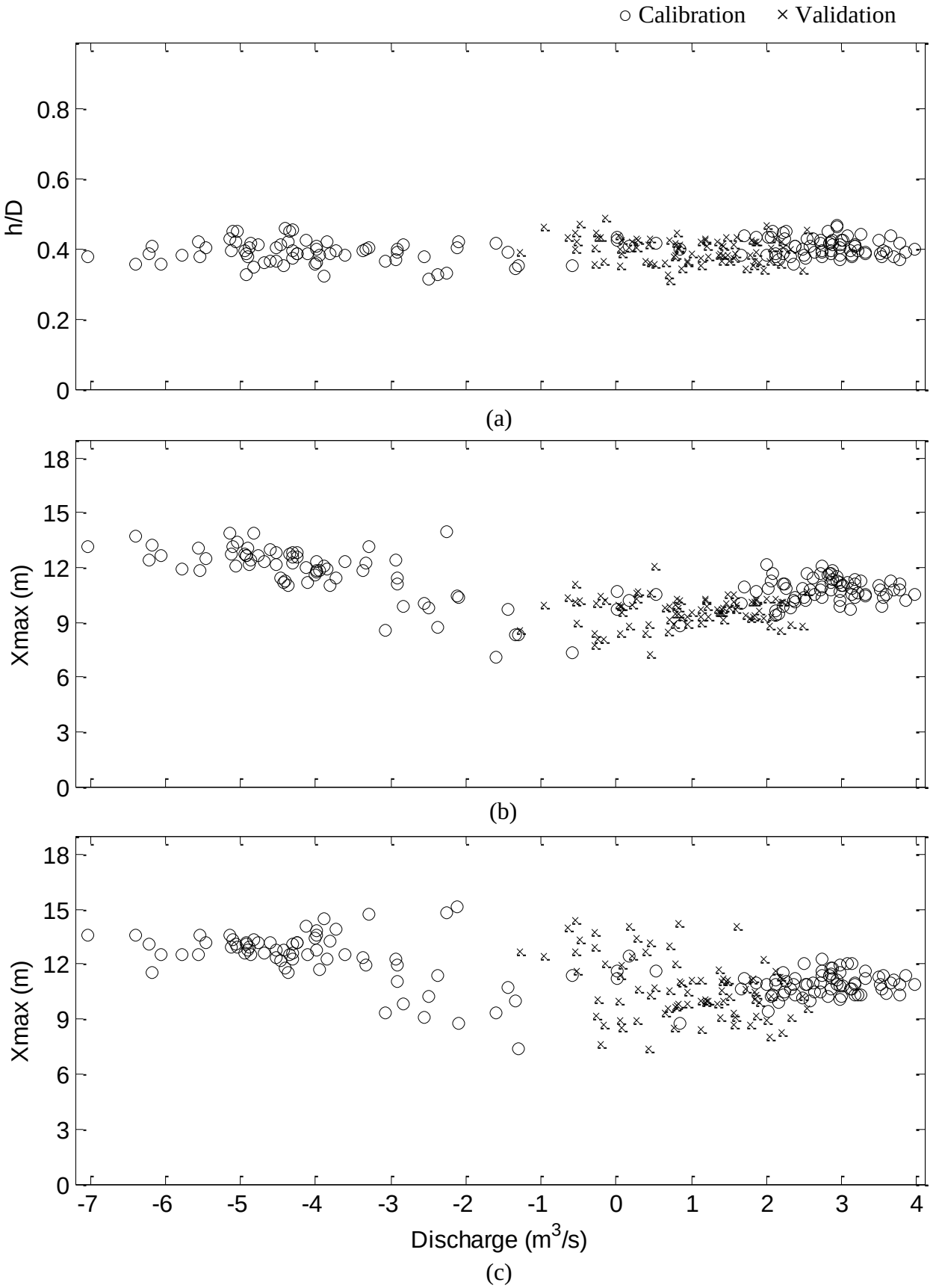

Figure 6: Plot of (a) h/D determined from VADCP data, (b) x_{max} determined from HADCP data, (c) x_{max} determined from VADCP data

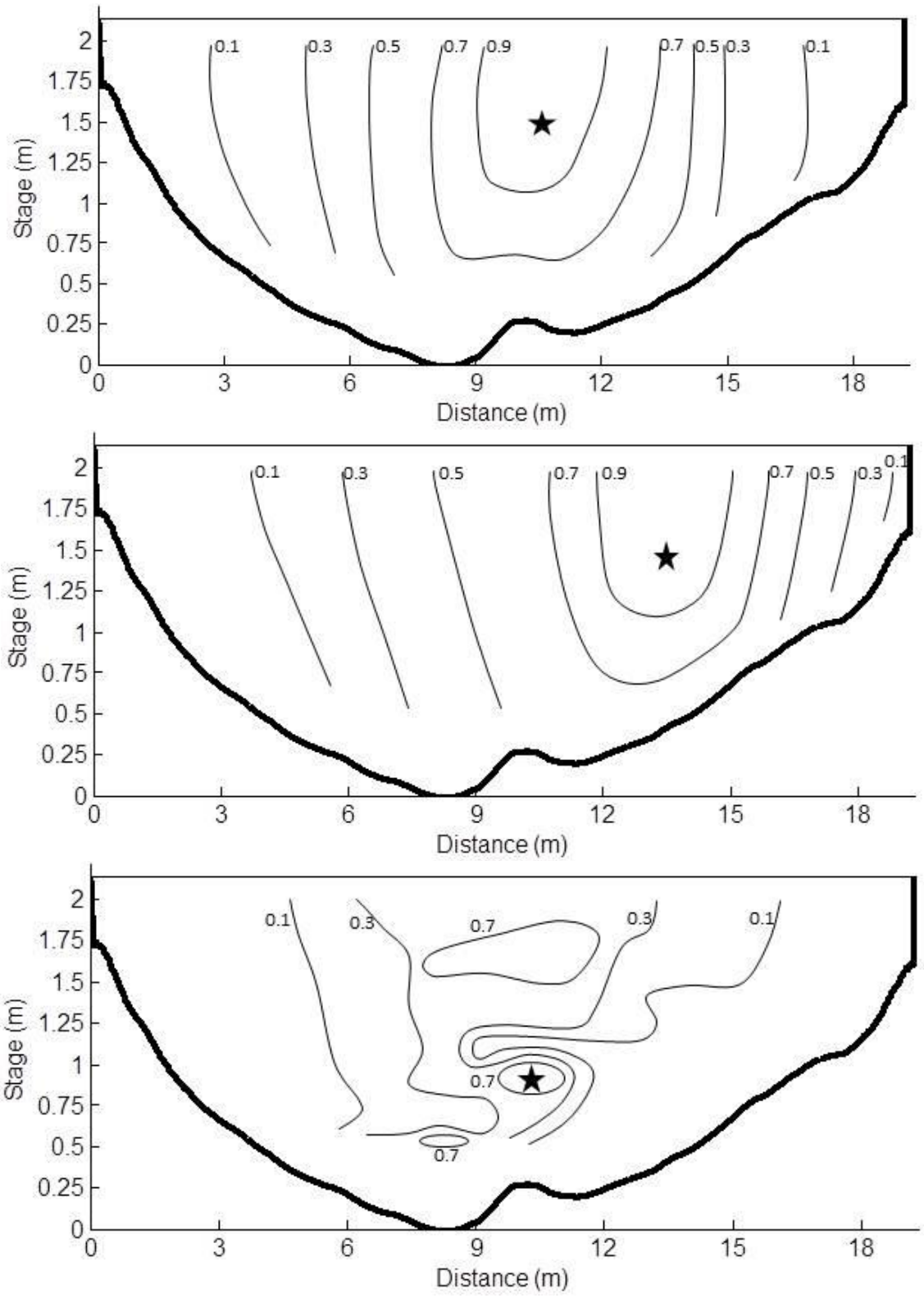

Figure 7: Relative velocity contours for positive flows (1 to 4 m^3/s), negative flow (-5 to -6.5 m^3/s), and low flows (0 to 1 m^3/s).

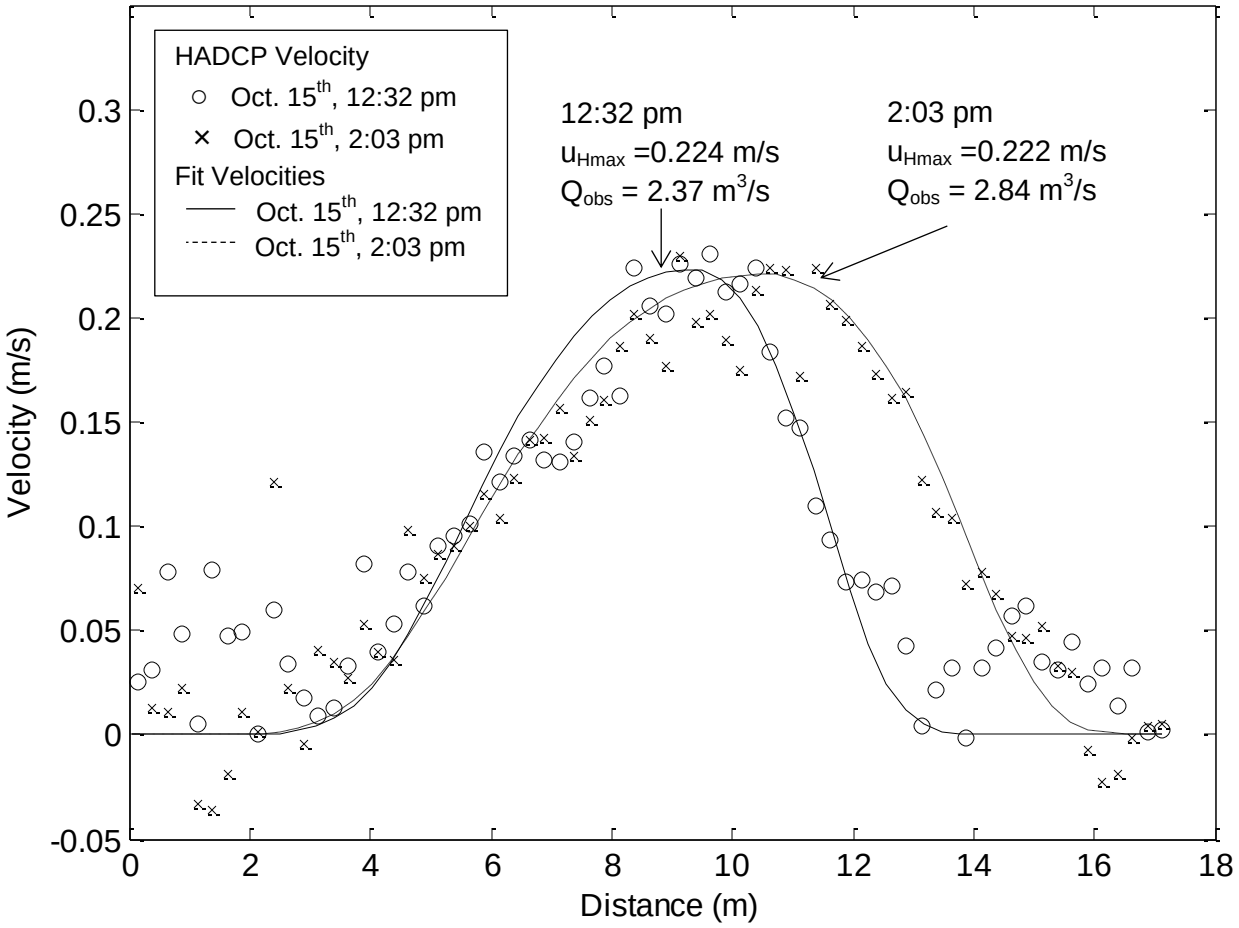

Figure 8: An example of an observed change in horizontal velocity distribution. Maximum velocities are similar, but discharges change significantly. Assuming a constant ratio between u_{max} and ū would not be appropriate for this case.

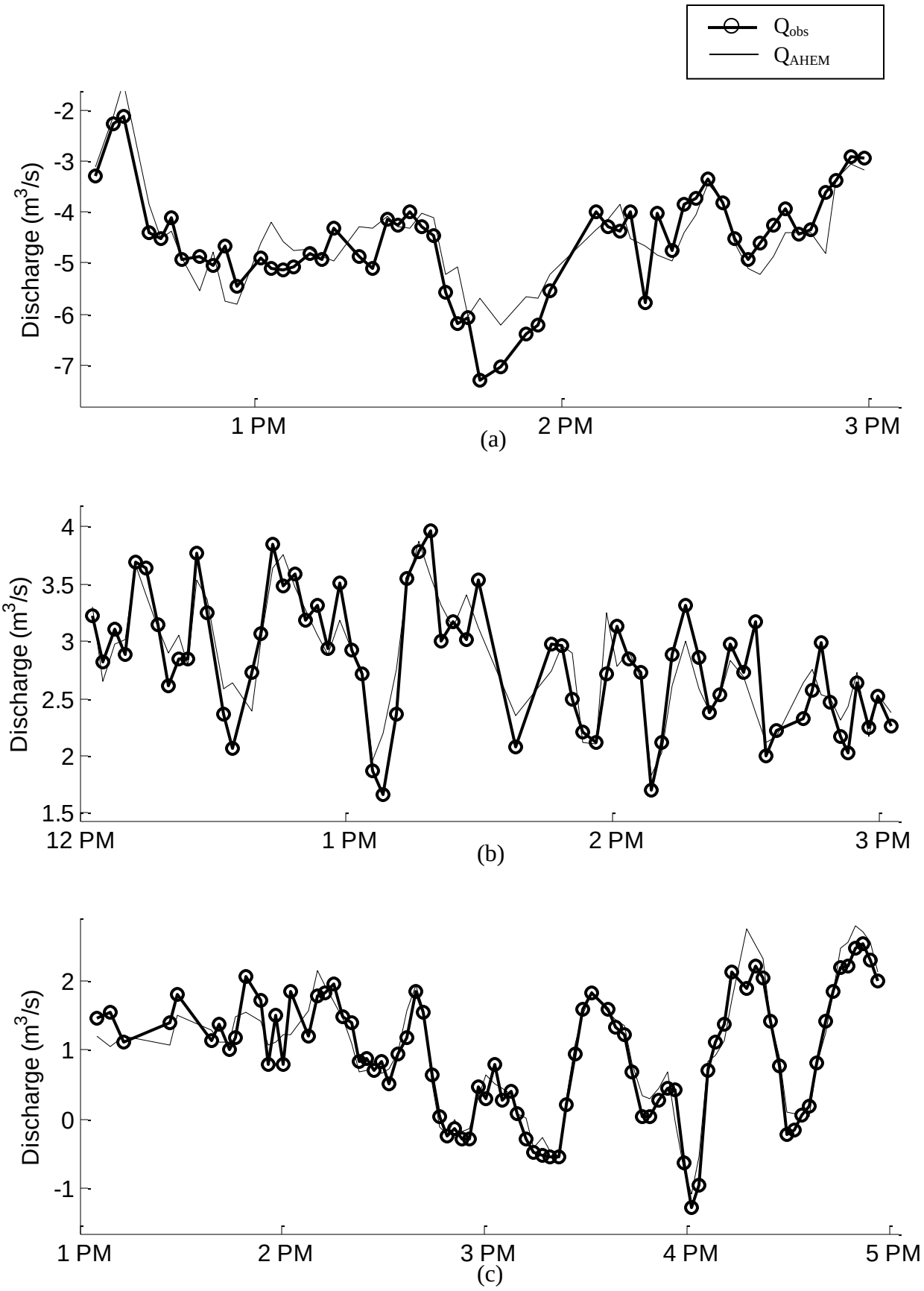

Figure 9: Measured and estimated discharge time series for three flow regimes: (a) negative, September 19th, (b) positive, October 15th, (c) transitional, October 24th (validation set)

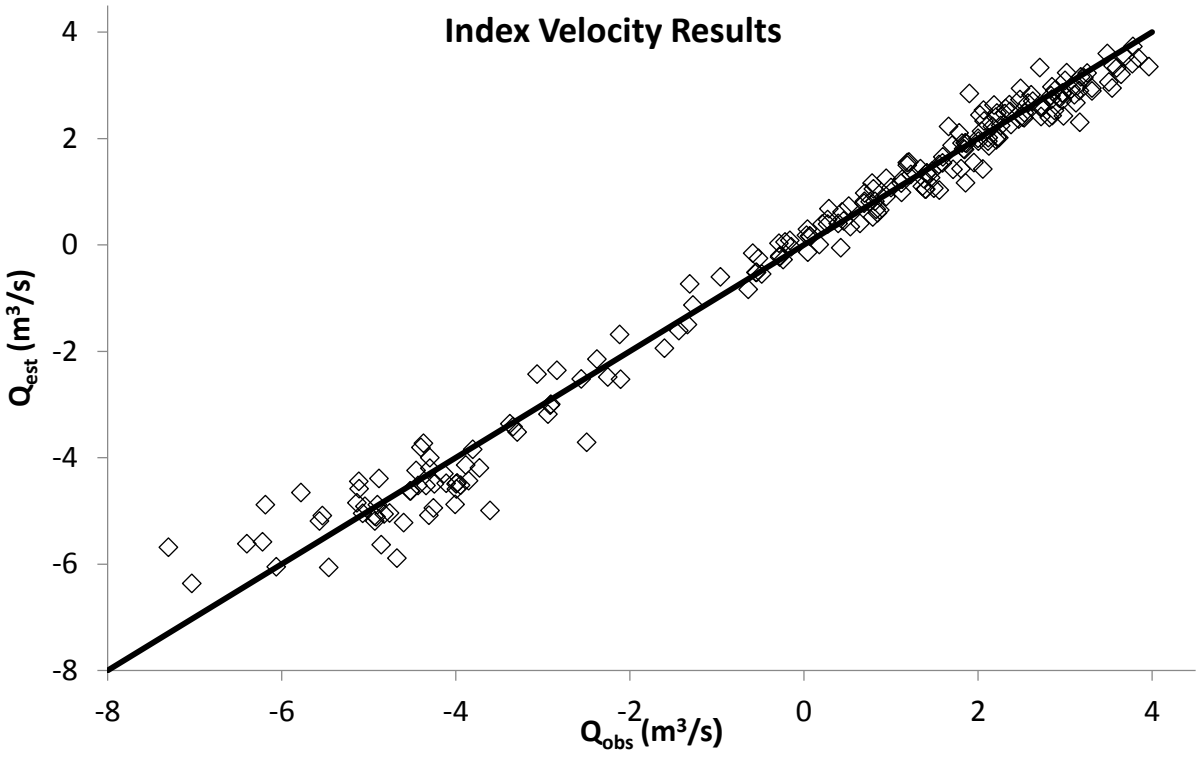

(a)

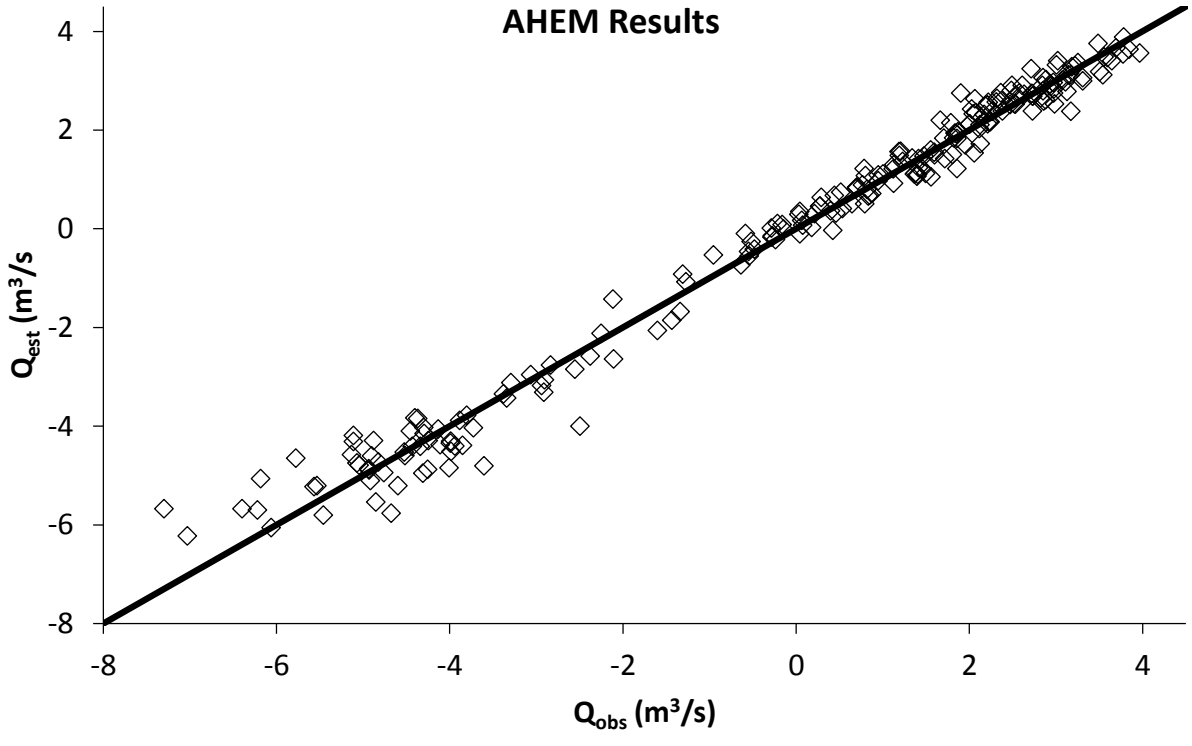

(b)

Figure 10: Q_{est} vs Q_{obs} when using the Index Velocity Method (a) and AHEM (b).

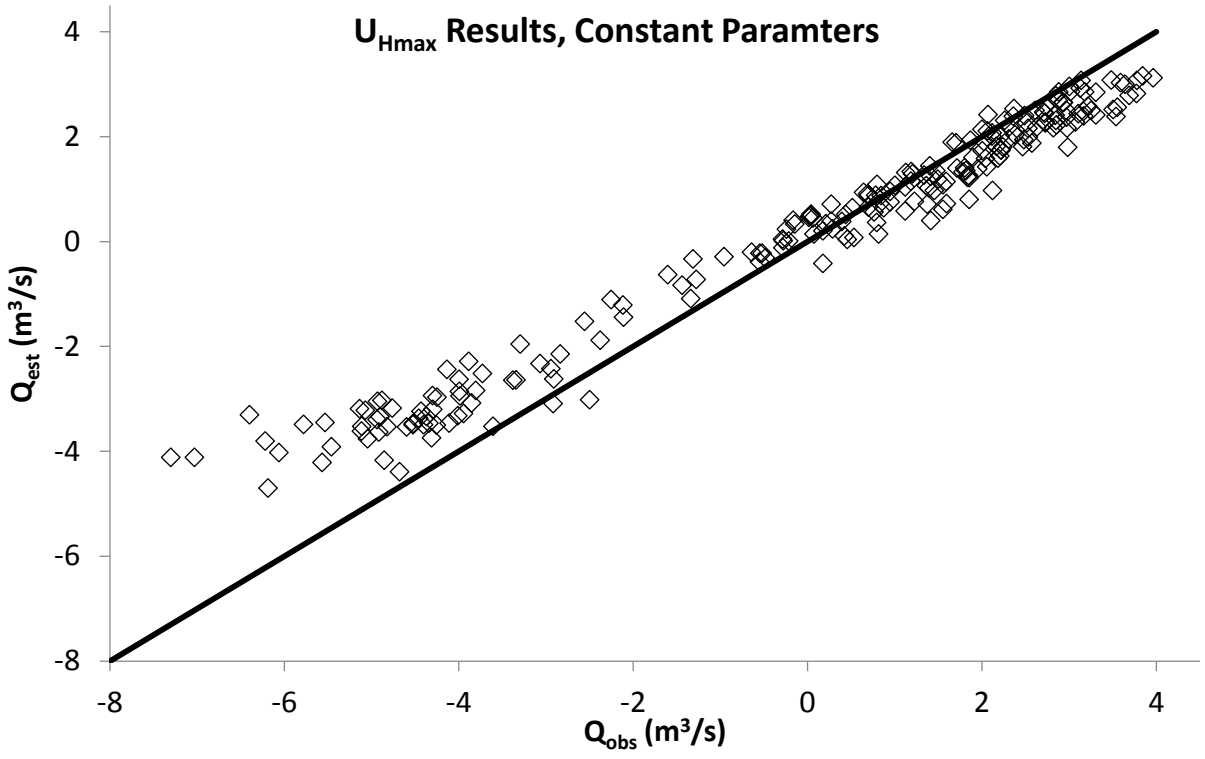

(a)

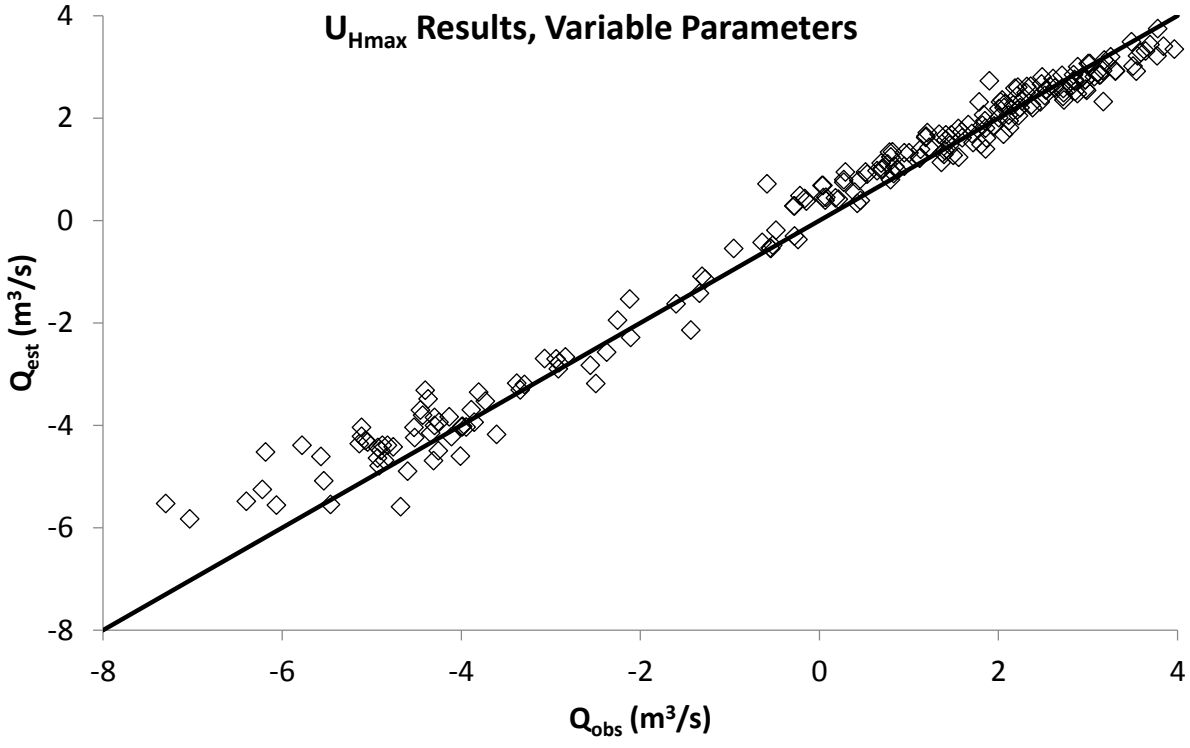

(b)

Figure 11: Q_{est} vs Q_{obs} when using AHEM with the maximum HADCP velocity (U_{Hmax}) and constant parameters (a) and variable parameters (b).

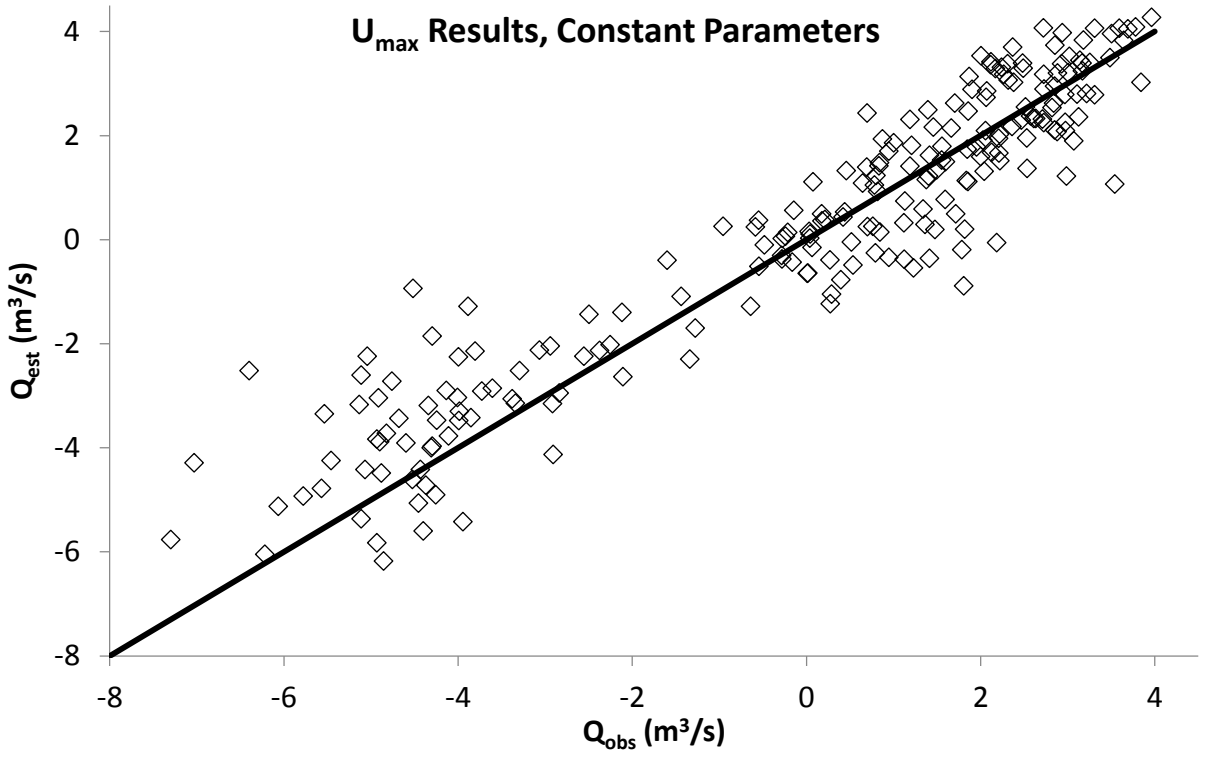

(a)

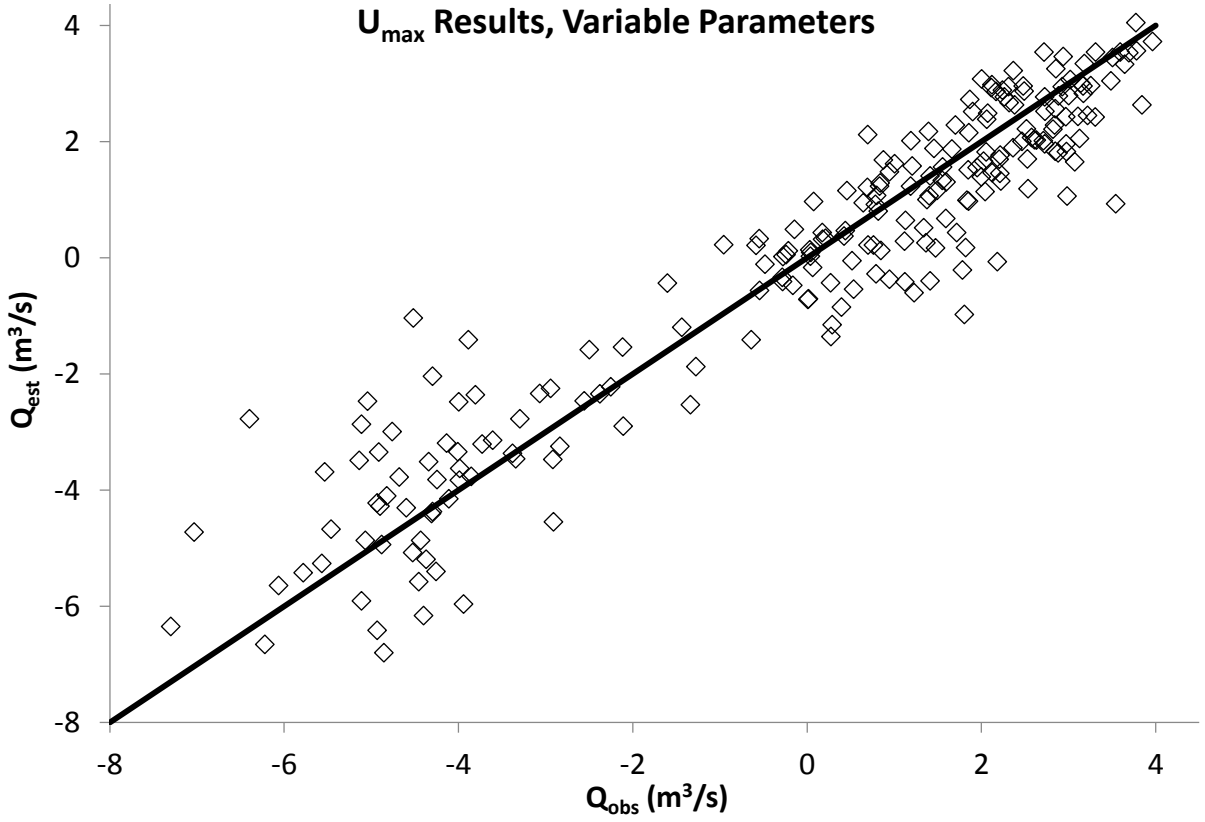

(b)

Figure 12: Q_{est} vs Q_{obs} when using conventional entropy with constant parameters (a) and variable parameters (b).

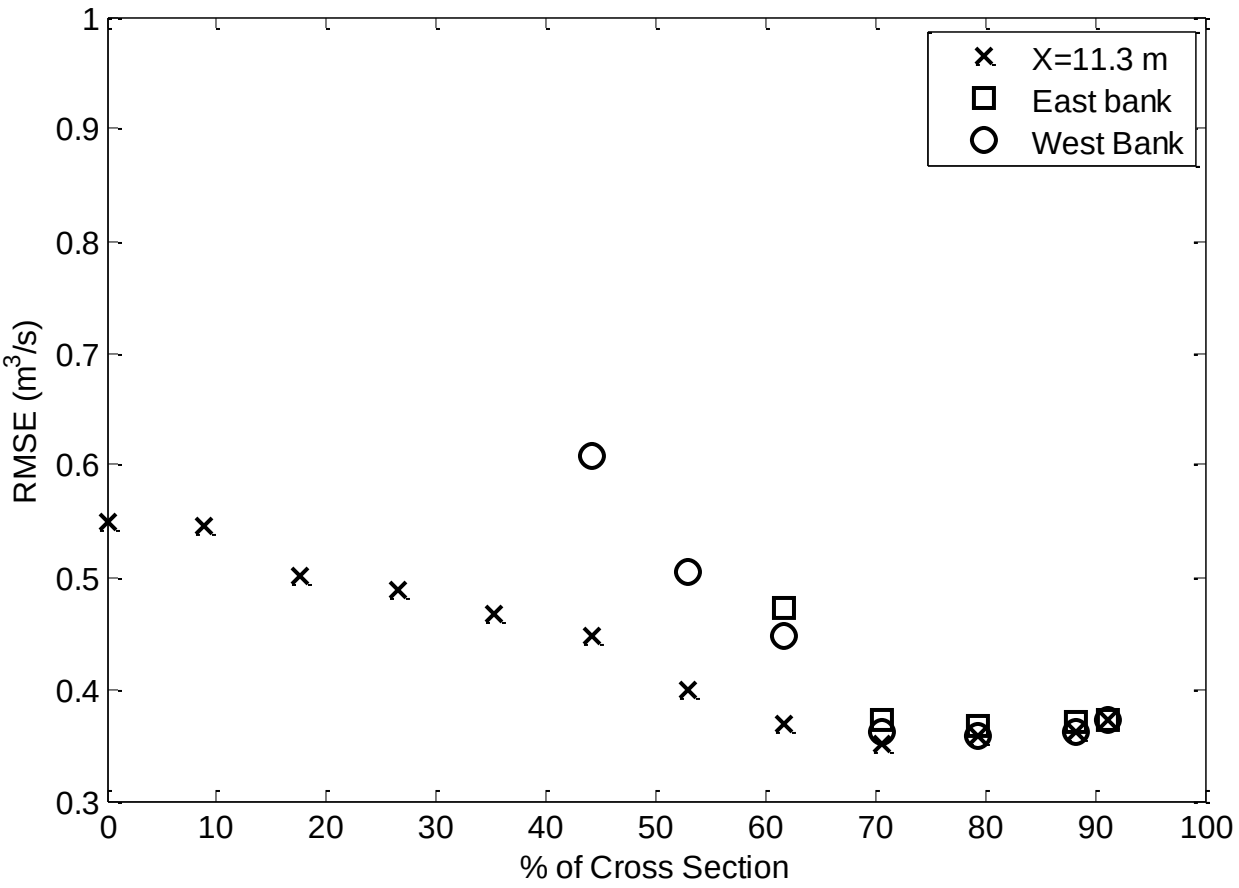

Figure 13: RMSE(m^3/s) is calculated as the percentage of measured cross section increases.